



Contents lists available at ScienceDirect

## Corrosion Science

journal homepage: [www.elsevier.com/locate/corsci](http://www.elsevier.com/locate/corsci)

## Letter

## EPMA and TEM characterization of intergranular tellurium corrosion of Ni–16Mo–7Cr–4Fe superalloy

Hongwei Cheng<sup>a,b</sup>, Bin Leng<sup>a,\*</sup>, Kai Chen<sup>c</sup>, Yanyan Jia<sup>a</sup>, Jiasheng Dong<sup>d</sup>, Zhijun Li<sup>a,\*</sup>, Xingtai Zhou<sup>a,\*</sup><sup>a</sup>Thorium Molten Salts Reactor Center, Shanghai Institute of Applied Physics, Chinese Academy of Sciences, Shanghai 201800, PR China<sup>b</sup>University of Chinese Academy of Sciences, Beijing 100049, PR China<sup>c</sup>State Key Laboratory for Mechanical Behavior of Materials, Xi'an Jiaotong University, Xi'an, Shanxi 710049, PR China<sup>d</sup>Institute of Metal Research, Chinese Academy of Sciences, Shenyang 110016, PR China

## ARTICLE INFO

## Article history:

Received 23 March 2015

Accepted 18 April 2015

Available online xxxx

## Keywords:

A. Superalloy

C. Intergranular corrosion

C. Reactor conditions

## ABSTRACT

The corrosion behavior of a Ni–16Mo–7Cr–4Fe alloy was investigated in a tellurium (Te) vapor atmosphere at 800 °C. Te was identified via electron probe microanalysis at the grain boundary regions of the corroded alloy. The morphology, chemical composition, and crystalline structure of those areas were characterized in a transmission electron microscope. Chromium tellurides were observed at both grain boundaries and intergranular carbide–matrix interfaces. Based on the results, the mechanism of intergranular Te corrosion and its possible correlation with intergranular cracking is discussed.

© 2015 Elsevier Ltd. All rights reserved.

## 1. Introduction

With the growing demands for safe, reliable, and economical nuclear energy, developing next generation nuclear reactors is attracting more and more interests and attentions. The molten salt reactor (MSR), which uses molten fluoride salts as coolant and dissolves fuel in the coolant, is one of the most promising next generation reactors due to its inherent safety, simplified fuel cycle, and high power generation efficiency [1,2]. Despite these advantages of MSRs, the high temperature molten fluoride salts environment brings great challenges to the corrosion resistance of MSR structural materials [3,4]. Some nickel-based superalloys possess good corrosion resistance against molten salts and small thermal expansion coefficients, thus are considered as the key engineering materials for various structural applications in MSRs [5,6]. In the 1950s and 1960s, Oak Ridge National Laboratory (ORNL), USA, designed and developed Alloy N (Hastelloy N), a Ni-based superalloy with moderate Cr content to reduce the molten fluoride salts corrosion and with high Mo content for solid solution strengthening, specifically for the molten salt test reactor. However, the intergranular cracking (IGC) of Hastelloy N has been observed during the operation of the test reactor [7]. Forming on the surface of the alloy,

intergranular cracks can deteriorate the mechanical properties of the structural components of the MSR, and further shorten their lifetime. Therefore, for the development of molten salt energy systems, it is important to understand the mechanism of the IGC [8]. Early studies by ORNL indicate that the cracks on the surface of Hastelloy N are mainly related to the inward diffusion of tellurium (Te), a fission product that can be dissolved in the salts and corrode the structural materials during the operation of the reactor [9,10]. According to those studies, Te induced IGC is possibly due to the formation of some brittle grain boundary (GB) compounds, whereas no direct observation of those compounds has been done to support the mechanism. Since the 1970s when ORNL stopped its MSR related research, the studies on Te-induced corrosion and cracking of Ni-based alloys have been ceased for decades. Recently, studies in this field have been revived because of the request of building next generation MSRs. Annealing experiments of Te electroplated pure Ni show that Te diffuses into Ni samples mainly along GBs at and below 900 °C [11]. Computer simulation results indicate that the segregation of Te at GBs induces GB expansion, thus weakens the interfacial Ni–Ni bonds which are essential to GB cohesion [12,13]. However, these studies do not provide the full description of the GB after Te corrosion. For instance, the exact morphology, chemical composition, as well as the structure of the segregated Te or tellurides are still unrevealed. Moreover, the previous discussion on the mechanism of Te-induced IGC is based on the simulations of pure Ni metals, without considering the effects of other alloy elements. This study is aiming at a complete characterization of the GBs of a Te corroded Ni-based superalloy. The

\* Corresponding authors at: 2019 Jia Luo Road, Jiading District, Shanghai Institute of Applied Physics, Chinese Academy of Sciences, Shanghai 201800, China. Tel.: +86 21 39194774; fax: +86 21 39194676.

E-mail addresses: [lengbin@sinap.ac.cn](mailto:lengbin@sinap.ac.cn) (B. Leng), [lizhijun@sinap.ac.cn](mailto:lizhijun@sinap.ac.cn) (Z. Li), [zhouxingtai@sinap.ac.cn](mailto:zhouxingtai@sinap.ac.cn) (X. Zhou).

mechanism of Te corrosion and its possible correlation with the IGC of the nickel-based superalloy are discussed.

## 2. Material and methods

The study was performed on alloy GH3535, a type of Alloy N with the nominal composition of Ni–16Mo–7Cr–4Fe (wt.%) that designed and fabricated in China specifically for the future applications of Chinese thorium molten salt reactor (TMSR). The original alloy bar (18 mm in diameter) was fabricated by casting and hot rolling (870 °C), followed by a solid solution treatment at 1177 °C for 0.5 h and water cooling. The chemical composition of the alloy was determined by inductively coupled plasma atomic emission spectroscopy, and is shown in Table 1. Specimens (1 mm in thickness) for tests were cut from the heat-treated bar. After that, the surfaces of the specimens were mechanically ground using SiC papers down to 1200 grit and washed with ethanol by ultrasonic bath for 20 min. Then each corrosion specimen was sealed in a vacuumed quartz tube (18 mm in diameter and 35 cm in length), along with a sufficient amount of Te powders (approximately 10 mg/cm<sup>2</sup> according to the size of specimen) to produce a Te vapor atmosphere. A comparison specimen was sealed in the same

type of vacuumed tube without Te powders to isolate the effect of annealing. After that, all tubes were kept in a muffle furnace at 800 °C for 100 h. The annealing temperature was chosen to meet the upper limit of the working temperatures of the structural materials (ranging from 700 to 800 °C depending on the locations of the structural components) in the future TMSR, for which this study is aiming to provide guidance.

After exposure, the corroded specimens were mounted in epoxy resin, wet ground with SiC papers down to 1200 grit, and polished to a 0.05 μm alumina paste finish, in order to prepare the cross-sectional samples for electron probe microanalysis (EPMA). Transmission electron microscope (TEM) samples were made near the corrosion surface by standard procedures: The corroded specimens were at first mechanically abraded down to about 100 μm in thickness, then punched into disks with a diameter of 3 mm, and finally electropolished in a solution of 5% HClO<sub>4</sub> and 95% CH<sub>3</sub>CH<sub>2</sub>OH at –30 °C using a TenuPol-5 twin-jet electro-polishing machine.

The elements distributions in cross-sectional samples were analyzed using a SHIMADZU 1720H EPMA, with an accelerating voltage of 25 kV and a beam current of 100 nA. The chemical composition and structure near the GB regions of the alloy after Te corrosion were investigated by a 200 kV FEI Tecnai G<sup>2</sup> F20

**Table 1**  
Chemical composition of the experimental alloy (wt.%).

Ni	Mo	Cr	Fe	Mn	Si	Al	C	Nb	P	S
Balance	15.9	6.88	4.1	0.49	1.01	0.88	0.05	0.01	0.003	0.003

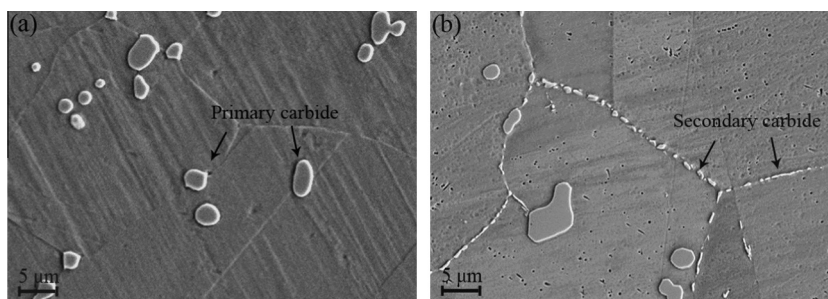


**Fig. 1.** Secondary electron images showing the microstructures of comparison specimen: (a) before annealing and (b) annealed at 800 °C for 100 h.

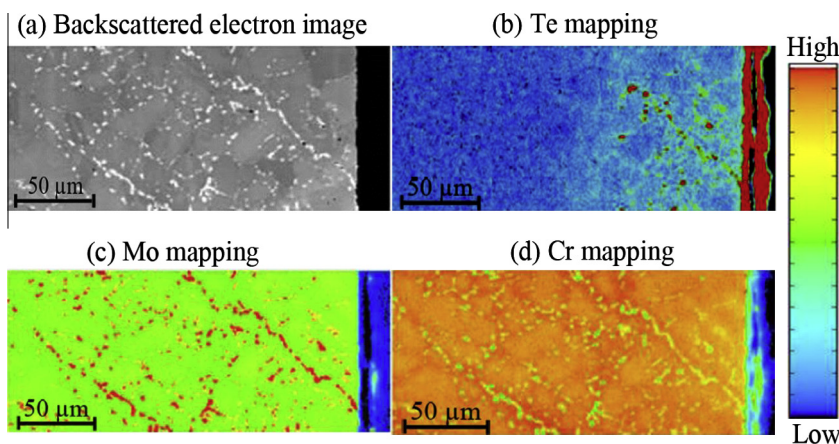


**Fig. 2.** (a) EPMA image of the cross-sectional specimen corroded by Te vapor at 800 °C for 100 h in backscattered electron mode and (b–d) elements distribution map of the same area. The surface of the specimen is to the right of the image (the color spectrum maps indicate levels of X-ray counts. Red and blue colors represent the highest and lowest counts, respectively). (For interpretation of the references to color in this figure legend, the reader is referred to the web version of this article.)

S-TWIN TEM with an energy dispersion spectrometer (EDS), in both TEM and scanning transmission electron microscope (STEM) modes.

### 3. Results and discussion

The microstructures of the comparison specimen before and after annealing are shown in Fig. 1. The microstructure of sample prior to heat treatment is characterized by some large precipitates that randomly distributed in the matrix (Fig. 1(a)). A previous study on Hastelloy N has shown that these precipitates are  $M_6C$  primary carbides, where M consists 27.9 wt.% Ni, 3.3 wt.% Si, 56.1 wt.% Mo and 4.0 wt.% Cr [14]. After annealing at 800 °C for 100 h, the grain size of the alloy and the morphology of the primary carbides remained almost the same, while some fine precipitates were observed at GBs (Fig. 1(b)). Previous investigations of this alloy have identified these fine precipitates as Mo-rich intergranular secondary carbides, which are also  $M_6C$  type [15,16].

The cross-section of the corroded specimen after annealing at 800 °C for 100 h in the Te vapor atmosphere was examined using EPMA, and presented in Fig. 2. The element mapping results show that Te exists at both the reaction layer on the specimen surface and the GBs up to about 110  $\mu\text{m}$  beneath the specimen surface (Fig. 2(b)). The reaction layer on the specimen surface consists of  $\text{CrTe}$  and  $\text{Ni}_3\text{Te}_2$  as identified by X-ray diffraction in the previous study [17]. The identification of Te at the GBs indicates that Te diffuses into the alloy mainly along GBs at this temperature, same as the diffusion behavior of Te in pure Ni [11]. Meanwhile, the extensive presence of the Mo-rich intergranular secondary carbides was also confirmed by the element mapping (Fig. 2(c)). However, from Fig. 2, it is difficult to tell whether Te is combined with Mo in those carbides or exists in the form of telluride at GBs. Therefore, EPMA analyses at higher magnification and more precise S/TEM analyses were performed and are presented in the next few paragraphs.

The high magnification EPMA analyses of the cross-section of the corroded specimen are shown in Fig. 3. The clusters of fine precipitates, which are distributed along GBs (Fig. 3(a)), can be clearly seen. The EPMA element mapping (Fig. 3(b)) and EDS point analyses (Fig. 3(c) and (d)) reveal that these precipitates are either Mo-rich or Te-rich. As discussed before, the Mo-rich phase is a  $M_6C$  intergranular secondary carbide. Semi-quantitative analysis of the Te-rich phase (Fig. 3(c)) shows that this phase contains 61.88 wt.% Te, 16.05 wt.% Cr, as well as some Ni and Mo. Considering the very small size of the Te-rich particle (about 1–3  $\mu\text{m}$ ), the detected Ni and Mo signals are possibly due to the surrounding Ni-rich matrix and the Mo-rich carbides. Therefore, the Te-rich phase is likely to be chromium telluride ( $\text{CrTe}$ ), which is the most stable telluride at temperatures above 750 °C according to the analyses of the surface reaction layers of Te corroded nickel-based alloys [18]. However, the accurate stoichiometry of this telluride was not determined here due to the uncertainty of EDS element quantification. All the Cr–tellurides in Fig. 3 are observed at GBs and located adjacent to intergranular carbides, which suggests that their formation can be ascribed to the inward diffusion of Te along the GBs and may have some correlations with the intergranular carbides. To further investigate the structure and composition of the tellurides, the GBs and intergranular carbides in the specimen after Te corrosion were examined with TEM/STEM.

The STEM high angle annular dark field (HAADF) image of a GB in the alloy after Te corrosion is shown in Fig. 4(a). A lath shaped phase of about 300 nm in width is observed at the GB. As is shown in the EDS mappings (Fig. 4(b)), the enrichment of Cr and Te in the lath shaped phase at the GB is observed, whereas the depletion of Cr is observed in the region surrounding the lath

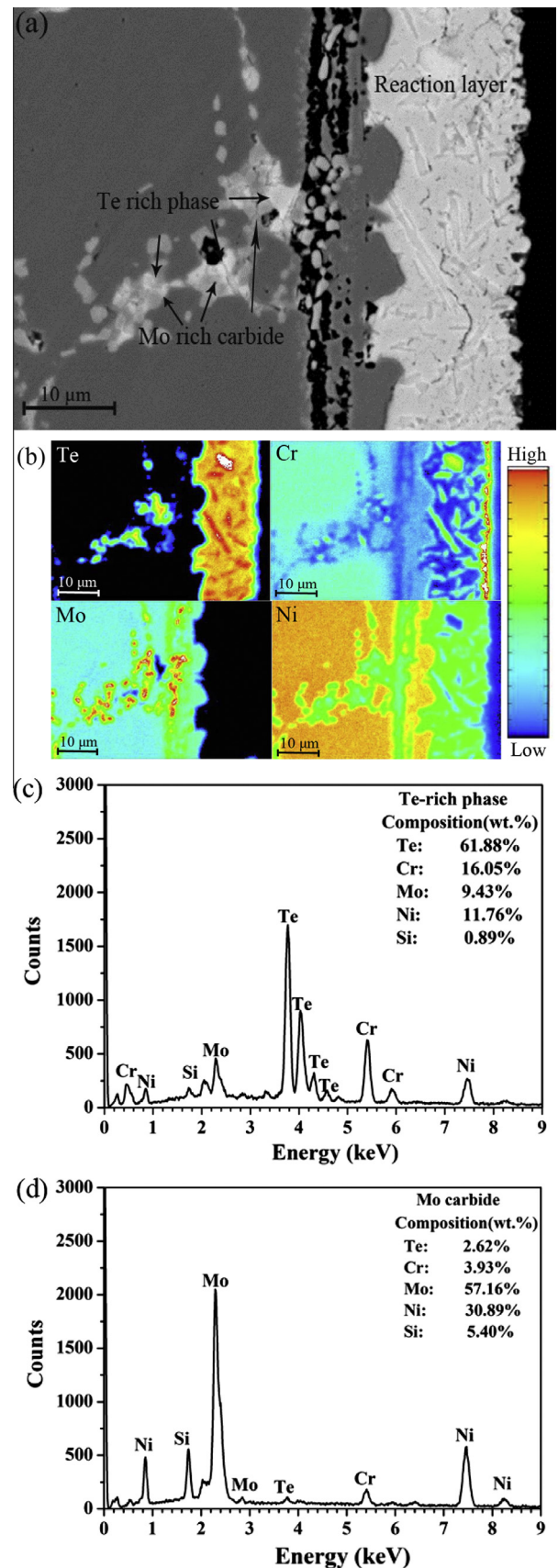
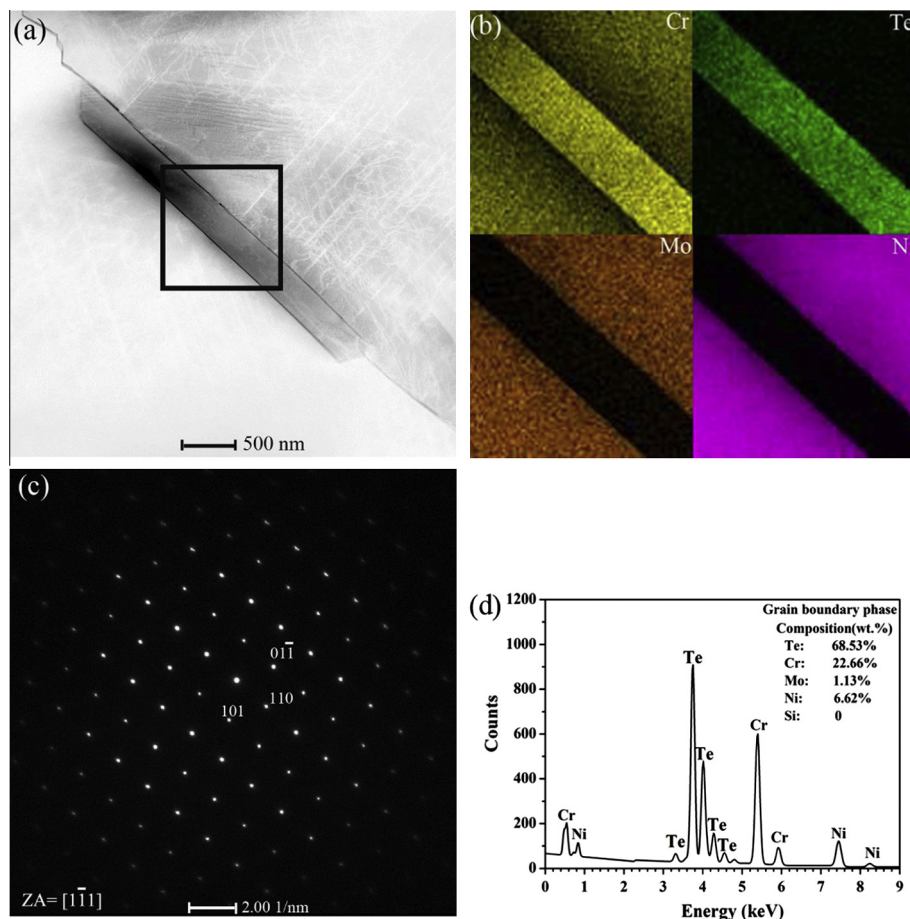


Fig. 3. EPMA analyses of the Te corroded sample at higher magnification: (a) microstructure (backscattered electron image); (b) EPMA mappings; (c) and (d) EDS spectra of Te-rich phase and Mo carbide, respectively.



**Fig. 4.** S/TEM analyses of a grain boundary phase in the Te corroded specimen: (a) STEM-HAADF image; (b) STEM-EDS mappings of the phase (area within the black box in (a)); (c) SAED pattern of the phase and (d) spectrum of EDS point analysis at the phase.

shaped GB phase, indicating that the phase is formed by the reaction of the inward diffused Te and the outward diffused Cr at the GB during annealing. The quantitative EDS analysis of the GB phase (Fig. 4(d)) yields a composition of about 22.66 wt.% Cr and 68.53 wt.% Te, corresponding to an atomic ratio of approximately 1:1, which reveals that the GB phase is CrTe. Considering the fact that the thickness of the GB phase is comparable to that of a TEM specimen (about 150 nm), the signal from the surrounding matrix is very low, and the result here should be more accurate than the EDS result of the bulk sample (Fig. 3(c)), and the identification of CrTe should be authentic. Careful indexing of the selected area electron diffraction (SAED) pattern (Fig. 4(c)) of the intergranular CrTe shows that it has a cubic structure with a lattice parameter of approximately 8.46 Å.

Besides being observed at GBs, CrTe could also be found near intergranular carbides, and an example is presented in Fig. 5. As is shown in Fig. 5(c), a thin layer with a zig-zag morphology is observed at the edge of an intergranular carbide. TEM-EDS analysis (spectrum 2 in Fig. 5(d)) shows that similar amounts of Cr and Te are presented in the layer, indicating that the thin layer phase is also CrTe. No Te is identified inside the carbide (spectrum 1 in Fig. 5(d)). Indexing of the SAED pattern (Fig. 5(b)) shows that the carbide has a face-centered cubic structure, which is the same as its original  $M_6C$  structure [15]. Therefore, it is reasonable to infer that intergranular carbides do not react with the inward diffused Te. Nevertheless, the interfaces between intergranular carbides and the alloy matrix, just like GBs, can act as preferential sites for accommodating Te and for Cr-Te reaction.

In light of the above results, the mechanism of intergranular Te corrosion of the Ni-based alloy can be described as follows: When annealed at 800 °C, Te diffuses into the alloy along GBs and can be accommodated at both GBs and intergranular carbide-matrix interfaces. Subsequently, the segregated Te at those sites can react with Cr from the adjacent areas to form cubic structure intergranular CrTe.

It has long been assumed that Te induced IGC of Ni-based alloys is due to the formation of certain brittle tellurides at the GBs [14]. However, none of such intergranular tellurides has been experimentally observed until this study. As an intermetallic compound, CrTe is intrinsic brittle. Therefore, the formation of CrTe at GBs and intergranular carbide-matrix interfaces will embrittle those sites, making them vulnerable to cracking. Meanwhile, the GB CrTe can immobilize the GB thus prevent the accommodation of GB sliding, which will induce stress localization and facilitate the originating of cracks [19]. Additionally, the formation of the zig-zag shaped CrTe at carbide-matrix interfaces roughens the interfaces. A previous study on Ni-based alloys with different carbide morphologies has shown that alloy with irregular shape carbide suffers from more severe cracking than alloy with round shape carbide [20]. Therefore, CrTe can also contribute to cracking by roughening the intergranular carbide-matrix interfaces. Despite of all these possibilities that CrTe can cause IGC in the Ni-based alloy, it is not conclusive that the formation of such intergranular compound is the main reason of the IGC observed in the real MSR since the Te concentration in this study is much higher than that of a real MSR environment [8]. Corrosion experiments of Ni-based alloys

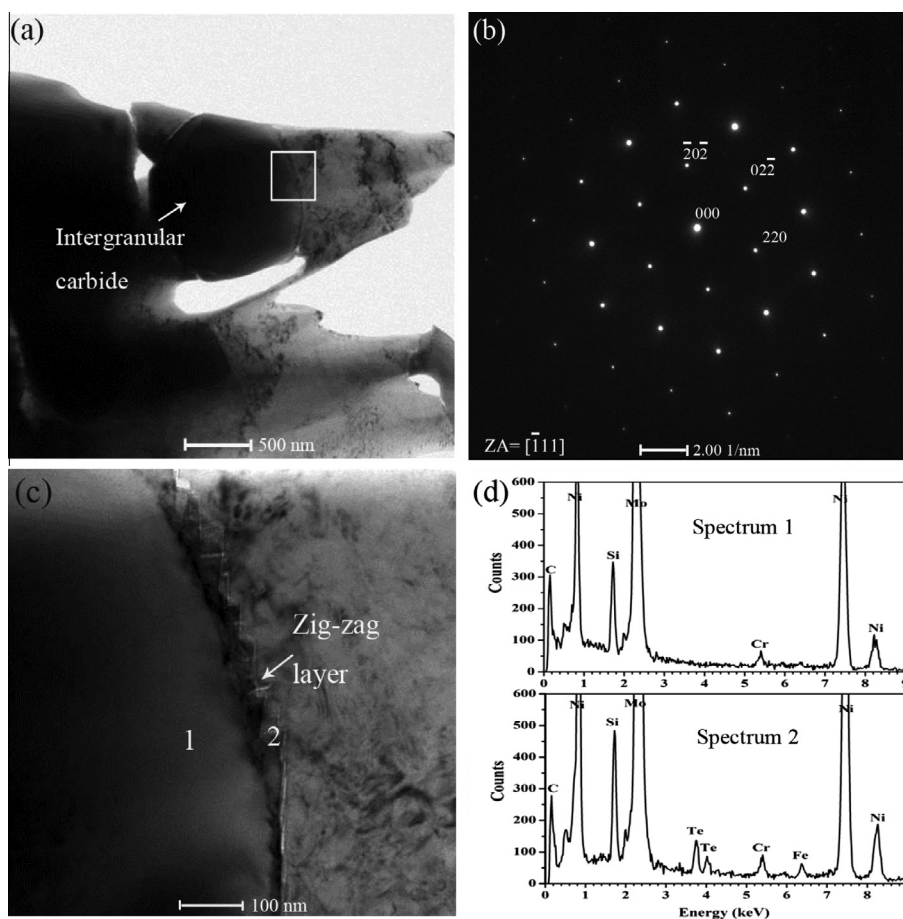


**Fig. 5.** TEM analyses of an intergranular carbide in the Te corroded specimen: (a) morphology of the carbide; (b) SAED patterns of the carbide (c) high magnification view of area within the white box in (a), showing a zig-zag layer formed at edge of the carbide and (d) spectra of EDS point analyses of the carbide and the zig-zag layer, respectively.

with different compositions in Te-containing molten salts have shown that the alloys with 7 wt.% and 15 wt.% Cr suffered same extent of Te-induced IGC while the alloy with 23 wt.% Cr suffered less, although no explanations are given to the results [14]. It might be possible that with the increasing of Cr content in the alloy, a protective Cr-telluride scale could form on the sample surface to prevent the further diffusion of Te into the alloy. However, the existence of such protective layer was neither confirmed in this study nor reported before. Therefore, whether Cr facilitates the Te-induced IGC or Cr prevents it should depend on the Cr content in the alloy and the Te content in the environment. Further investigations including corrosion experiments with different Cr and Te concentrations and mechanical tests are needed to elucidate this point.

#### 4. Conclusions

In summary, the distribution of Te in a Ni–16Mo–7Cr–4Fe alloy after annealing at 800 °C for 100 h in a Te vapor atmosphere has been investigated. Te exists at the GB regions up to about 110 μm beneath the sample surface, indicating that Te penetrates into the alloy by an intergranular diffusion mechanism. The characterizations of the morphology, chemical composition and crystalline structure of those Te containing regions show that a cubic structure CrTe can form at GBs and the interfaces between intergranular carbides and the alloy matrix. The results imply that Te corrosion occurs through the reaction between Te and Cr at the intergranular sites when Te diffuses into the alloy along GBs at

elevated temperature. The formation of such telluride can possibly induce intergranular cracking of the alloy.

#### Acknowledgements

This work is supported by the Program of International S&T Cooperation, ANSTO-SINAP (Grant No. 2014DFG60230), the National Natural Science Foundation of China (Grant No. 51371188), the Science and Technology Commission of Shanghai Municipality (Grant No. 11JC1414900), the Strategic Priority Research Program of the Chinese Academy of Sciences (Grant No. XDA02004210), the National Young 1000 Talents Program of China, and the Fundamental Research Funds for the Central Universities (Grant No. 2015GJHZ03).

#### References

- [1] J. Uhler, *Chemistry and technology of molten salt reactors history and perspectives*, *J. Nucl. Mater.* 360 (2007) 6–11.
- [2] D. LeBlanc, *Molten salt reactors: a new beginning for an old idea*, *Nucl. Eng. Des.* 240 (2010) 1644–1656.
- [3] E. Mohammadi Zahrani, A.M. Alfantazi, *Molten salt induced corrosion of Inconel 625 superalloy in PbSO<sub>4</sub>–Pb<sub>3</sub>O<sub>4</sub>–PbCl<sub>2</sub>–Fe<sub>2</sub>O<sub>3</sub>–ZnO environment*, *Corros. Sci.* 65 (2012) 340–359.
- [4] Hanliang Zhu, Rohan Holmes, Tracey Hanley, Joel Davis, Ken Short, Lyndon Edwards, *High-temperature corrosion of helium ion-irradiated Ni-based alloy in fluoride molten salt*, *Corros. Sci.* 91 (2015) 1–6.
- [5] R.C. Reed, *The Super Alloys: Fundamentals and Applications*, Cambridge University Press, New York, 2006.
- [6] Sung-Il Baik, M.J. Olszta, S.M. Bruemmer, David N. Seidman, *Scr. Mater.* (2012) 809–812.

- [7] J.R. Keiser, Status of tellurium-Hastelloy N studies in molten fluoride salts, ORNL/TM-6002, Oak Ridge, TN, USA, 1977, pp. 1–23.
- [8] V. Ignatiev, A. Surenkov, Ivan Gnidoy, Alexander Kulakov, Vadim Uglov, Alexander Vasiliev, Mikhail Presniakov, Intergranular tellurium cracking of nickel-based alloys in molten Li Be Th U/F salt mixture, *J. Nucl. Mater.* 440 (2013) 243–249.
- [9] M.W. Rosenthal, R.B. Briggs, Molten-Salt Reactor, ORNL/TM-4832, Oak Ridge, TN, USA, 1973, pp. 1–13.
- [10] H.E. McCoy, Intergranular Cracking of Structural Materials Exposed to Fuel Salt, ORNL/TM-4782, 1972, pp. 128–136.
- [11] Yanyan Jia, Hongwei Cheng, Jie Qiu, Fenfen Han, Yang Zou, Zhijun Li, Xingtai Zhou, Hongjie Xu, Effect of temperature on diffusion behavior of Te into nickel, *J. Nucl. Mater.* 441 (2013) 372–379.
- [12] W. Liu, H. Han, Cuilan Ren, Xiujie He, Yanyan Jia, Song Wang, Wei Zhang, Zhijun Li, Xingtai Zhou, Yang Zou, Ping Huai, Hongjie Xu, First-principles study of intergranular embrittlement induced by Te in the Ni  $\Sigma$ 5 grain boundary, *Comput. Mater. Sci.* 88 (2014) 22.
- [13] M. Všiánska, M. Šob, The effect of segregated sp-impurities on grain-boundary and surface structure, magnetism and embrittlement in nickel, *Prog. Mater. Sci.* 56 (2011) 817–840.
- [14] H.E. Mc Coy, Status of materials development for molten salt reactors [R], ORNL/TM-5920, Oak Ridge, TN, USA, 1978.
- [15] Zhoufeng Xu, Jiang Li, Jiasheng Dong, Zhijun Li, Xingtai Zhou, The effect of silicon on precipitation and decomposition behaviors of  $M_6C$  carbide in a Ni–Mo–Cr superalloy, *J. Alloys Compd.* 620 (2015) 197–203.
- [16] X.L. Li, S.M. He, X.T. Zhou, Y. Zou, Z.J. Li, A.G. Li, X.H. Yu, Effects of rare earth yttrium on microstructure and properties of Ni–16Mo–7Cr–4Fe nickel-based superalloy, *Mater. Charact.* 95 (2014) 171–179.
- [17] Hongwei Cheng, Fenfen Han, Yanyan Jia, Zhijun Li, Xingtai Zhou, Effects of Te on intergranular embrittlement of a Ni–16Mo–7Cr alloy, *J. Nucl. Mater.* 461 (2015) 122–128.
- [18] R.E. Gehlbach, H. Henson, Identification from Tellurium-Structure-Material interaction, ORNL/TM-4832, Oak Ridge, TN, USA, 1972, pp. 79–89.
- [19] D.A. Woodford, Gas phase embrittlement and time dependent cracking of nickel based superalloys, *Energy Mater.* (2006) 59–79.
- [20] X.M. Guan, H.Q. Ye, Intergranular embrittlement caused by the precipitation of  $M_6C$  carbide containing silicon, *J. Mater. Sci.* 15 (1980).